

# Nanosecond laser induced damage in RbTiOPO<sub>4</sub>: The missing influence of crystal quality

Anne Hildenbrand,<sup>1</sup> Frank R. Wagner,<sup>1,\*</sup> Jean-Yves Natoli,<sup>1</sup> and Mireille Commandré<sup>1</sup>

<sup>1</sup>Institut Fresnel, CNRS, Aix-Marseille Université, Ecole Centrale Marseille, Campus de Saint-Jérôme, 13013  
Marseille, France

\*frank.wagner@fresnel.fr

**Abstract:** Nanosecond laser induced damage in RbTiOPO<sub>4</sub> (RTP) an isomorphous material to the more widely known KTiOPO<sub>4</sub> (KTP) is studied in crystals with varying properties. The ionic conductivity along the z-axes of the tested crystals ranged from  $1.5 \cdot 10^{-9}$  S/cm to  $1.1 \cdot 10^{-12}$  S/cm. Further, different growth sectors with different absorption in the range of hundreds of ppm/cm and differing zones in inhomogeneous crystals have been investigated. Despite these important differences in crystal quality, no significant difference could be observed in the laser damage resistance at 1064 nm. Thus growth induced defects only play a minor role in nanosecond laser induced damage in RTP. Transient, laser induced defects are discussed in analogy with KTP as possible laser damage precursors.

©2009 Optical Society of America

OCIS codes: (140.3330) Laser damage; (190.4400) Nonlinear optics, materials; (230.2090) Electro-optical devices.

## References and links

1. M. Roth, M. Tseitlin, and N. Angert, "Oxide crystals for electro-optic Q-switching of lasers," *Glass Phys. Chem.* **31**(1), 86–95 (2005).
2. R. C. Eckardt, H. Masuda, Y. X. Fan, and R. L. Byer, "Absolute and Relative Nonlinear Optical Coefficients of KDP, KD\*P, BaB<sub>2</sub>O<sub>4</sub>, LiIO<sub>3</sub>, MgO-LiNbO<sub>3</sub>, and KTP Measured by Phase-Matched 2nd-Harmonic Generation," *IEEE J. Quantum Electron.* **26**, 922–933 (1990).
3. M. Tseitlin, E. Mojaev, and M. Roth, "Growth of high resistivity RbTiOPO<sub>4</sub> crystals," *J. Cryst. Growth* **310**(7-9), 1929–1933 (2008).
4. S. Wang, V. Pasiskevicius, and F. Laurell, "Dynamics of green light-induced infrared absorption in KTiOPO<sub>4</sub> and periodically poled KTiOPO<sub>4</sub>," *J. Appl. Phys.* **96**(4), 2023–2028 (2004).
5. B. Jacobsson, V. Pasiskevicius, F. Laurell, E. Rotari, V. Smimov, and L. Glebov, "Tunable narrowband optical parametric oscillator using a transversely chirped Bragg grating," *Opt. Lett.* **34**(4), 449–451 (2009).
6. J. Chen, A. J. Pearlman, A. Ling, J. Y. Fan, and A. L. Migdall, "A versatile waveguide source of photon pairs for chip-scale quantum information processing," *Opt. Express* **17**(8), 6727–6740 (2009).
7. M. Munowitz, R. H. Jarman, and J. F. Harrison, "Theoretical Study of the Nonlinear-Optical Properties of KTiOPO<sub>4</sub> - Effects Of Ti-O-Ti Bond Angles and Oxygen Electronegativity," *Chem. Mater.* **5**, 1257–1267 (1993).
8. V. Murk, V. Denks, A. Dudelzak, P. P. Proulx, and V. Vassiltchenko, "Gray tracks in KTiOPO<sub>4</sub>: Mechanism of creation and bleaching," *Nucl. Instrum. Methods Phys. Res. B* **141**(1-4), 472–476 (1998).
9. Y. Jiang, L. E. Halliburton, M. Roth, M. Tseitlin, and N. Angert, "EPR and ENDOR study of an oxygen-vacancy-associated Ti<sup>3+</sup> center in RbTiOPO<sub>4</sub> crystals," *Physica B* **400**(1-2), 190–197 (2007).
10. A. Hildenbrand, F. R. Wagner, H. Akhouayri, J. Y. Natoli, M. Commandré, F. Théodore, and H. Albrecht, "Laser-induced damage investigation at 1064 nm in KTiOPO<sub>4</sub> crystals and its analogy with RbTiOPO<sub>4</sub>," *Appl. Opt.* **48**(21), 4263–4269 (2009).
11. F. Wagner, A. Hildenbrand, J. Y. Natoli, M. Commandré, F. Theodore, and H. Albrecht, "Laser damage investigation in KTiOPO<sub>4</sub> (KTP) and RbTiOPO<sub>4</sub> (RTP) crystals: Threshold anisotropy and the influence of SHG," *Proc. SPIE* **6720**, 672015 (2007).
12. S. Favre, T. C. Sidler, and R. P. Salathe, "High-power long-pulse second harmonic generation and optical damage with free-running Nd:YAG laser," *IEEE J. Quantum Electron.* **39**(6), 733–740 (2003).
13. H. Yoshida, H. Fujita, M. Nakatsuka, M. Yoshimura, T. Sasaki, T. Kamimura, and K. Yoshida, "Dependences of laser-induced bulk damage threshold and crack patterns in several nonlinear crystals on irradiation direction," *Jpn. J. Appl. Phys.* **45**, 766–769 (2006).
14. F. R. Wagner, A. Hildenbrand, J.-Y. Natoli, M. Commandré, F. Theodore, and H. Albrecht, "Laser damage resistance of RbTiOPO<sub>4</sub>: evidence of polarization dependent anisotropy," *Opt. Express* **15**, 13849–13857 (2007).

15. S. Verma, and P. J. Shlichta, "Imaging techniques for mapping solution parameters, growth rate, and surface features during the growth of crystals from solution," *Prog. Cryst. Growth Charact. Mater.* **54**(1-2), 1–120 (2008).
16. G. S. Settles, "Shadowgraph Techniques," in *Schlieren and Shadowgraph Techniques: Visualizing Phenomena in Transparent Media* (Springer, 2001), p. 143.
17. A. Alexandrovski, G. Foulon, L. E. Myers, R. K. Route, and M. M. Fejer, "UV and visible absorption in  $\text{LiTaO}_3$ ," *Proc. SPIE* **3610**, 44–51 (1999).
18. M. Roth, N. Angert, M. Tseitlin, and A. Alexandrovski, "On the optical quality of KTP crystals for nonlinear optical and electro-optic applications," *Opt. Mater.* **16**(1-2), 131–136 (2001).
19. A. Hildenbrand, F. R. Wagner, H. Akhouayri, J.-Y. Natoli, and M. Commandré, "Accurate metrology for laser damage measurements in nonlinear crystals," *Opt. Eng.* **47**(8), 083603 (2008).
20. L. Gallais, and J. Y. Natoli, "Optimized metrology for laser-damage measurement: application to multiparameter study," *Appl. Opt.* **42**(6), 960–971 (2003).
21. International Organization of, Standardization, "Determination of laser-damage threshold of optical surfaces Part 2: S-on-1 test," (ISO 11254-2, 2001), p. 29.
22. L. Lemaître, S. Bouillet, R. Courchinoux, T. Donval, M. Josse, J. C. Poncetta, and H. Bercegol, "An accurate, repeatable, and well characterized measurement of laser damage density of optical materials," *Rev. Sci. Instrum.* **78**(10), 103105 (2007).
23. J. Y. Natoli, B. Bertussi, and M. Commandré, "Effect of multiple laser irradiations on silica at 1064 and 355 nm," *Opt. Lett.* **30**(11), 1315–1317 (2005).
24. H. Krol, L. Gallais, C. Grèzes-Besset, J.-Y. Natoli, and M. Commandré, "Investigation of nanoprecursors threshold distribution in laser-damage testing," *Opt. Commun.* **256**(1-3), 184–189 (2005).
25. R. A. Negres, N. P. Zaitseva, P. DeMange, and S. G. Demos, "Expedited laser damage profiling of  $\text{KD,H}_{2-3}\text{PO}_4$  with respect to crystal growth parameters," *Opt. Lett.* **31**(21), 3110–3112 (2006).

## 1. Introduction

Rubidium titanyl phosphate,  $\text{RbTiOPO}_4$  (RTP), and the isomorphic material potassium titanyl phosphate,  $\text{KTiOPO}_4$  (KTP), are well established nonlinear optical materials for electro optic applications and frequency conversion respectively [1,2]. Recent advances in the elaboration of high quality RTP [3] and the better understanding of photo-induced effects in KTP [4] show the continuing scientific and technological interest in these materials. Two modern applications for periodically poled KTP should be mentioned: (i) tunable near infrared sources, e.g [5], and (ii) the generation of identical photons for quantum optics experiments, e.g [6].

From the beginning of the frequent usage of KTP in the early 1990ies, the high nonlinear coefficient and the gray tracks appearing during frequency doubling of Nd:YAG lasers motivated a lot of fundamental and applied studies on this material and its isomorphs [7,8]. Comparisons of RTP and KTP always pointed out the strong similarity of these materials. In particular the problematic color centers and the laser damage properties are very similar [9–11].

In this article the infrared nanosecond laser damage phenomenon in RTP in a configuration similar to its usage in Pockels cells will be addressed and an interpretation of the measurements, based on the analogy between RTP and KTP, will be proposed. Statistical laser damage tests have been carried out in different growth sectors exhibiting different infrared absorption levels within the same crystal. Further, crystals from two different providers with different ionic conductivities have been tested. The missing influence of these parameters on the laser induced damage statistics gives insight concerning the laser damage mechanism in RTP, and, by analogy, KTP.

Some detailed investigations on nanosecond laser damage in KTP and RTP exist [12–14]. The damage initiation mechanism is either suspected to be linked to the color centers that cause the gray-track phenomenon [10,12], or dielectric breakdown caused by self-focusing is considered [13].

## 2. Samples

Sample 1, a 34 mm x 34 mm y-cut sample with a thickness of 10 mm, was made from a standard flux by provider  $\alpha$  and has been used in order to investigate the influence of the infrared absorption level on the nanosecond laser induced damage. Figure 1 shows the optical shadowgraph [15,16] of the sample.



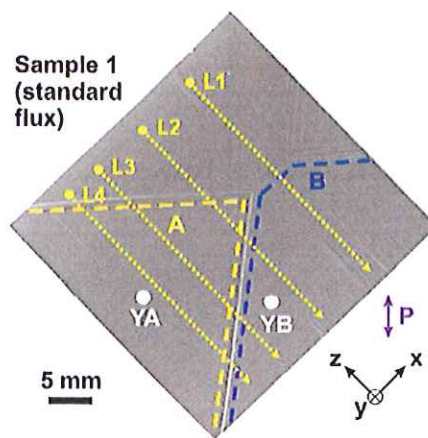


Fig. 1. Optical shadowgraph of sample 1 (y-cut, 34 mm x 34 mm x 10 mm). Different growth sectors can be distinguished as partially indicated by the dashed lines. Few visible defects are present within a given growth sector. Laser damage tests have been performed in sectors A and B using a polarization along P. Infrared absorption measurements have been performed along the dotted lines L1-L4 and at locations YA and YB (see Fig. 2).

The homogeneous growth sectors A and B show different infrared absorption (Fig. 2) as measured by photothermal common-path interferometry [17]. The (linear) absorption of sector A at the damage testing wavelength is approximately 1.6 to 2 times higher than the absorption of sector B. It indicates different amounts of growth induced crystal defects in both zones as for example contamination by other elements.

Two more, smaller y-cut samples (sample 2 and 3, 10 mm x 10 mm x 10 mm), originating from experimental fluxes from provider  $\alpha$ , have also been used to study the influence of growth induced crystal defects. The shadowgraphs in Fig. 3 indicate the zones used for laser damage testing. The zones delimited in these samples are not necessarily different growth sectors, but lines in the optical shadowgraphs indicate discontinuities in the crystal composition or the concentration of crystal defects (dislocations etc). In fact the lines in the shadowgraphs are caused by discontinuities of the complex index resulting in wavefront distortions.

The other samples from provider  $\alpha$  (from the standard flux, like sample 1) and provider  $\beta$  (sample 4), all x-cut, 4 mm x 4 mm in size and 10 mm long were homogeneous.

The macroscopic ionic conductivities along the z-axis for the different types of samples have also been measured and are given in Table 1. The ionic conductivity is given as one of the parameters for estimating the gray-track resistance of KTP crystals [18] or the susceptibility to electrostatic darkening in RTP [3].

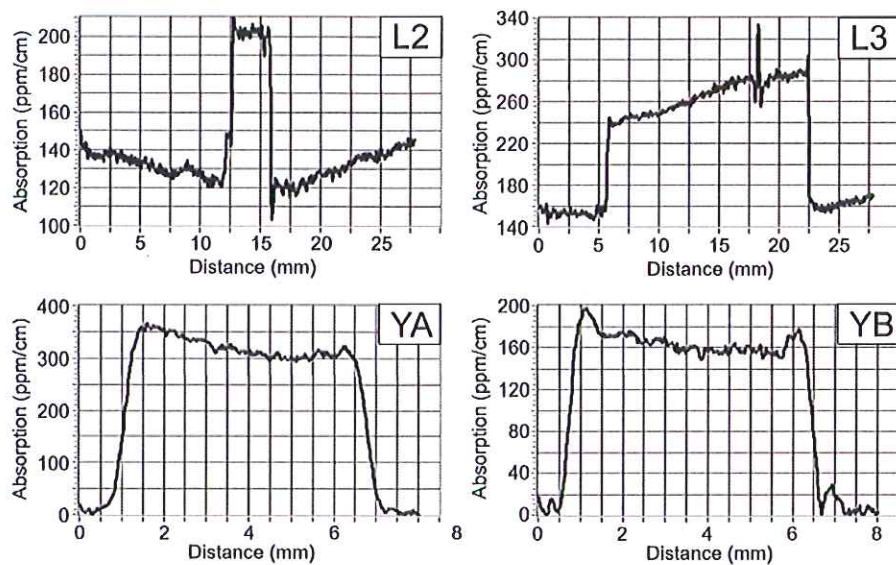


Fig. 2. Infrared absorption measurements of sample 1 by the photothermal lensing method: L2 and L3 are line scans along the z-axis of the crystal. YA and YB are in-depth scans along the y-axis of the crystal. (See Fig. 1 for the locations.) Sector A has a 1.6-2 times higher absorption as sector B. The distances in traces YA and YB indicate the sample displacement and have to be multiplied with the refractive index in order to convert them to physical coordinates in the crystal.

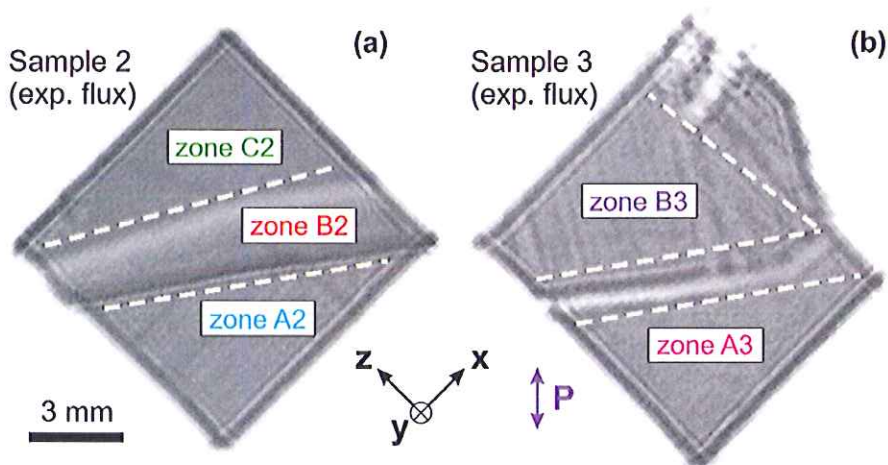


Fig. 3. Optical shadowgraph of sample 2 and 3 (y-cut, 10 mm x 10 mm x 10 mm). Different zones can be distinguished as indicated by the dashed lines. Each zone is characterized by a certain type of defects as sensed by optical shadowgraphy.

**Table 1. Ionic conductivities along the z-axis and fluxes used for the growth of the samples**

Sample	Provider	Typical conductivity along z-axis	Flux
Sample 1	$\alpha$	$1.5 \cdot 10^{-9}$ S/cm	$\text{Rb}_6\text{P}_4\text{O}_{13}$
Sample 2	$\alpha$	$8.0 \cdot 10^{-10}$ S/cm	$\text{Rb}_5\text{P}_4\text{O}_{13}$
Sample 3	$\alpha$	$5.5 \cdot 10^{-10}$ S/cm	$\text{Rb}_4\text{P}_4\text{O}_{13}$
Sample 4	$\beta$	$1.1 \cdot 10^{-12}$ S/cm	self-flux

### 3. Laser induced damage measurements

#### 3.1. Experimental setup and procedure

A schematic of the experimental setup is shown in Fig. 4. A Q-switched Nd:YAG laser (1064 nm, 6 ns, 10 Hz pulse repetition rate) is used to initiate laser induced damage by focusing the radiation to a spot diameter of  $75 \mu\text{m}$  ( $1/e^2$ , Gaussian beam profile). The laser beam is parallel within the 10 mm thick sample, and for RTP (and KTP) damages appear distributed over a large range of depth values in the bulk of the crystal. Using a parallel beam places us in conditions similar to the operating conditions of the crystals and avoids focusing aberrations [19]. The polarization for all tests is at  $45^\circ$  to the z-axis of the crystals, similar to the incoming radiation in Pockels cells.

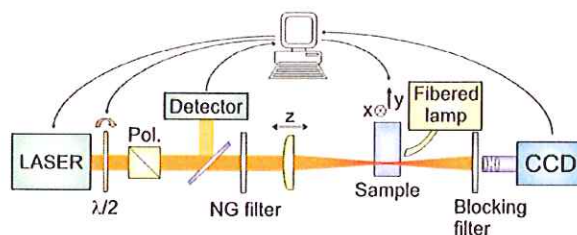


**Fig. 4. Schematic of the laser damage measurement setup.** A Quantel Ultra GRM laser (1064nm, 6ns, 10Hz) is focused on the sample. Damage detection is performed by imaging of backscattered light with high depth of field and subsequent image processing.

For RTP (and KTP), damages appear as micrometer sized cracks along the principal axis. Damage detection was performed by imaging of backscattered light (delivered by a fibered halogen lamp) and subsequent image processing [20]. The laser damage tests have been conducted in 200-on-1 mode, *i.e.* up to 200 pulses were used per site [21]. The test sites are spaced by  $400 \mu\text{m}$  in both transversal directions in order to obtain statistically independent results. The damage probability is estimated from the number of damaged sites divided by the number of tested sites. Due to the limited surface for some of the measurements (see for example zone B2 on sample 2) the number of used test sites per fluence varies within one series and thus the uncertainty of the damage probability varies within one series. The damage probability curves also give the 68%-confidence error which has been calculated according to [19]. A typical fluence error bar (not shown in the graphs) is 10% [22].

For comparison, the front surface threshold of a silica sample is  $60 \text{ J/cm}^2$  with a spot size of  $75 \mu\text{m}$ . A measurement in 2005, using a similar setup, yielded a silica surface damage threshold of  $65 \text{ J/cm}^2$  with a spot size of  $8 \mu\text{m}$  [23]. Both measurements have been performed in 1-on-1 mode.

#### 3.2. Damage probability curves

The damage probability curves that have been acquired on y-cut RTP crystals are shown in Fig. 5. Figure 5a compares the growth sectors A and B on sample 1, and, considering the scattering of the experimental data and the error bars, no significant difference has been found. Figure 5b compares the fit shown in Fig. 5a to the measurements in the samples 2 and



3. In Fig. 5b too, within the scattering of the data points and the error bars, samples 2 and 3 as well as the different zones in these samples cannot be distinguished. The repeated fit allows us to more easily compare the data points in Fig. 5a to the ones in Fig. 5b, and once again no significant differences are observed.

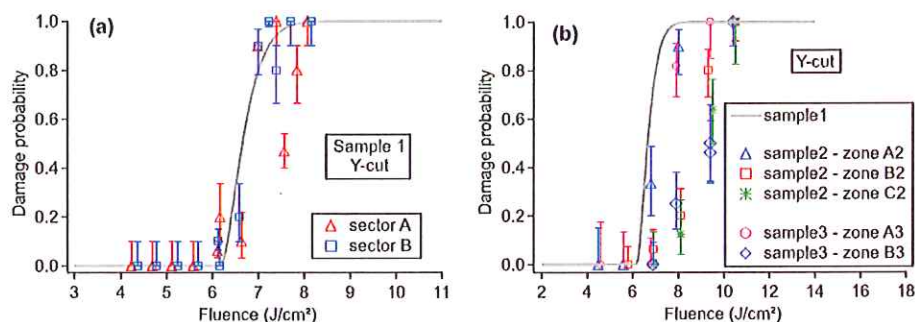


Fig. 5. Damage probability curves in 200-on-1 mode in y-cut RTP using a polarization at  $45^\circ$  to the crystal z-axis. Figure a: Comparison of the growth sectors A and B in sample 1. The solid line is a fit to the data using the Gaussian model [24]. Figure b: Comparison of the different zones in samples 2 and 3 to the fit of the data in Fig. 5a.

Figure 6 compares the laser damage probability curves of the x-cut RTP crystals. The sample from provider  $\alpha$  has been grown identically to sample 1 and shows thus the highest measured ionic conductivity. The sample from provider  $\beta$  is sample 4 and shows a factor of 1000 lower ionic conductivity (Table 1). Nevertheless the curves of both samples superpose. (The twofold increase in the damage threshold of the x-cut crystals with respect to the y-cut crystals has been discussed in [14].)

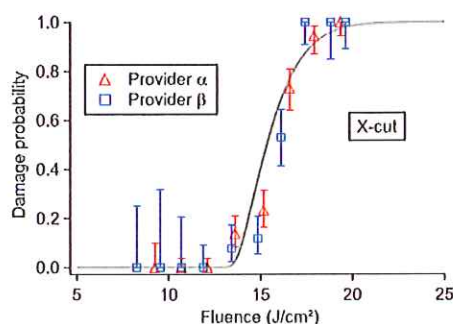


Fig. 6. Damage probability curves in 200-on-1 mode in x-cut RTP using a polarization at  $45^\circ$  to the crystal z-axis. The sample from provider  $\beta$  has much lower ionic conductivity than the one from provider  $\alpha$ . The solid line is again a fit to the data using the Gaussian model [24].

#### 4. Results and discussion

In summary, an independence of the nanosecond laser induced damage threshold of RTP on the growth induced crystal defects, within certain limits, is reported. In particular, a variation of the ionic conductivity from  $1.5 \cdot 10^{-9}$  S/cm to  $1.1 \cdot 10^{-12}$  S/cm, does not significantly decrease the laser damage performance with a longitudinal multimode Q-switched Nd:YAG laser at the fundamental wavelength of 1064nm. Neither do absorption variations of the laser wavelength from 130 ppm/cm to 320 ppm/cm. We may note that a similar behavior has been observed in DKDP [25].

In the following, we will try to understand these observations in RTP by considering an analogy with KTP where more detailed literature is available. In 2004, Wang *et al.* [4] reported on the dynamics of color center annealing after irradiation with different intensities at 532nm. They found that the relative importance of growth-related color centers decreases with increasing laser intensity. The offered explanation is that high light intensities induce the generation of unstable color centers which add to the growth related color centers. Additionally, Wang *et al.* propose a possible mechanism for the light induced generation of these unstable color centers. They consider that high intensity light may generate Frenkel defect pairs ( $V(K^+) - K_i^+$ ) having an estimated lifetime of 1-10 ms at 295K [8]. During the lifetime of the defect pair, a color center can then be formed close to the potassium vacancy. However, these light induced color centers annihilate rapidly once the potassium vacancy is occupied again. Hence, a fast spontaneous reduction of the green induced infrared absorption is observed [4]. As the lifetime of these unstable  $V(K^+)-K_i^+$ -pairs is presumably much longer than the pulse length in our setup (6 ns), they may act as laser damage precursors. Our results thus indicate that the laser damage mechanism at high intensities and relatively low pulse numbers is dominated by generated, unstable color centers, in contrast to growth-related, stable color centers.

The remaining question is how the unstable color centers are produced. RTP and KTP both show very high nonlinear optical properties and in consequence shorter wavelengths are produced. The generated visible and ultra-violet photons favor the electronic excitation of the material and thus the population of excited states in the quasi-conduction band. In the laser damage experiments we always observed some green light after the crystal when the fluence was approaching the damage threshold. Comparing in particular the case of x-cut and y-cut RTP tested with 45° polarization, mismatched type II second harmonic generation is about 5.8 times stronger in y-cut RTP than in x-cut RTP, a fact that concords with the observed laser damage threshold difference (Fig. 6 and Fig. 5) [14]. Considering the low energy that is necessary to create a  $V(K^+)-K_i^+$ -pair in KTP (1.4 eV [4]), it is clear that defect pairs can be generated with high efficiency by electrons relaxing from the quasi-continuum states of the conduction band. Phase matching greatly increases the production yield of energetic photons and thus the generation of excited electrons, but even in strongly mismatched situations energetic photons are produced locally at the distorted Ti-O-bond [7].

We thus suspect that nanosecond laser induced damage in RTP is mediated by the generation of unstable  $V(K^+)-K_i^+$ -pairs. Their generation in turn is a consequence of the combination of the high optical nonlinearity and the ease of Frenkel-pair generation in these materials.

The above discussion should not make us forget that many applications, e.g. tight focusing, are sensitive to wavefront distortions. Further, applications at lower intensities and high pulse numbers are sensitive to the growth induced crystal defects causing electrostatic darkening in RTP and gray-tracking in KTP.

## 5. Conclusions

We showed that nanosecond laser induced damage in RTP, as tested in a Pockels cell configuration, is independent on significant variations in crystal quality (ionic conductivity, infrared absorption, structural defects). This indicates that the laser damage precursors of this material are not growth dependent. Thus we conclude that the laser damage precursors are produced by photon induced processes during the pulse. In analogy with green induced infrared absorption measurements in KTP [4], we propose the light induced generation of unstable  $V(K^+)-K_i^+$ -pairs as a possible mechanism. These defect pairs, which may be generated by relaxing electronic excitation, are likely to be caused indirectly by frequency doubled photons that were always visible in our experiments.

The nanosecond laser induced damage threshold of RTP at low pulse numbers is thus limited by inherent material properties and the usage of the crystal (phase matching).

### **Acknowledgements**

We acknowledge Fred Theodore from Cristal Laser S.A. for the crystal characterization measurements and Hassan Akhouayri for valuable discussions and correction reading. The work has been funded by the Délégation Générale pour l'Armement (DGA) and the Centre National d'Etudes Spatiales (CNES).